

# Cosmic String Cusps with Small-Scale Structure: Their Forms and Gravitational Waveforms

Xavier Siemens

*Center for Gravitation and Cosmology, Department of Physics,  
University of Wisconsin — Milwaukee, P.O. Box 413, Wisconsin, 53201, USA*

Ken D. Olum

*Institute of Cosmology, Department of Physics and Astronomy, Tufts University, Medford, MA 02155, USA*  
(Dated: October 30, 2018)

We present a method for the introduction of small-scale structure into strings constructed from products of rotation matrices. We use this method to illustrate a range of possibilities for the shape of cusps that depends on the properties of the small-scale structure. We further argue that the presence of structure at cusps under most circumstances leads to the formation of loops at the size of the smallest scales. On the other hand we show that the gravitational waveform of a cusp remains generally unchanged; the primary effect of small-scale structure is to smooth out the sharp waveform emitted in the direction of cusp motion.

PACS numbers: 11.27.+d,98.80.Cq

## I. INTRODUCTION

The study and detection of gravitational waves is a very active area of current research. Gravitational radiation is a direct test of dynamical gravity and elucidating its properties experimentally has the potential to confirm (or even change) our current gravitational theory. Furthermore, the detection of a gravitational wave background would open a new observational window onto a time in the early universe much earlier than that of recombination, beyond which the universe is opaque to electromagnetic waves. The potential rewards to cosmology that would result from such a detection are countless. With the new interferometric gravitational wave telescopes (LIGO, GEO and TAMA) now operating and plans for a future space-based telescope (LISA) it will become possible to detect waveforms from various astrophysical sources, including topological defects. This has the potential to determine, or at worst constrain, the types of high energy particle theories that describe our world.

Topological defects are a prediction of most particle physics models that involve a symmetry breaking phase transition [1, 2] as well as some brane-world scenarios [3] and are therefore quite generic. Cosmic strings, in particular, have drawn considerable attention because they do not cause cosmological disasters and are good candidates for a variety of interesting cosmological phenomena such as gamma ray bursts [4], gravitational wave bursts [5] and ultra high energy cosmic rays [6].

Analytic studies [7, 8] and numerical simulations [9, 10, 11] show that cosmic string networks evolve toward an attractor solution known as the “scaling regime”. In this regime the energy density of the string network is a small constant fraction of the radiation or matter density and the statistical properties of the system such as the

correlation lengths of long strings and average sizes of loops scale with the cosmic time  $t$ . This solution is possible because of intercommutations that produce cosmic string loops which in turn decay by radiating gravitationally.

Simulations also have found that the perturbations on long strings and most loops have the smallest possible size, the simulation resolution, which does not scale. This small-scale structure arises from a build-up of the sharp edges (kinks) [12] produced at string intersection events and the initial Brownian character of the network. It is not clear, however, how very small loops can be formed at late times. The mechanism that has so far been suggested is that they form at regions of the string known as cusps [13], although in this case we expect the loops formed to have relativistic speeds. This is discussed at some length below. It may also be that the small loops form from the collapse of horizon-sized loops. The size of this small-scale structure is also thought to scale with the cosmic time  $t$ . The value typically quoted in the literature, first proposed in [14], is  $\Gamma G\mu t$ , where  $\Gamma$  is a number of order 100,  $G$  is Newton’s constant and  $\mu$  is the mass per unit length of the string, but the actual value may be many orders of magnitude smaller [15].

One of the key signatures of cosmic strings is the production of gravitational waves [16]. The network of long strings and loops is expected to produce a gravitational wave background as well as bursts coming from cusps and kinks. These bursts stand out of the gravitational wave background and may be detectable with current sensitivities [5].

In this paper we investigate the shape and gravitational waveforms of cusps with small-scale structure. In the next section we review the motion of strings and construct solutions where helical small-scale structure is introduced using products of rotations. In Section

III we investigate various small-scale structure regimes and show that the presence of small-scale structure at cusps under most circumstances leads to the production of loops at the size of the smallest scales. We further illustrate the various regimes, and shapes of the resulting cusps, using the solutions found in Section II. In Section IV we describe the numerical algorithm employed to compute gravitational waveforms and in Section V we show the waveforms for cusps on loops with and without small-scale structure. We conclude in Section VI.

## II. STRING MOTION

When the typical length scale of a cosmic string is much larger than its thickness, and long-range interactions between different string segments can be neglected, the string can be accurately modeled by a one-dimensional object. Such an object sweeps out a two-dimensional surface in space-time referred to as the string world-sheet. Here we will consider the motion of strings in flat space, which is a good approximation to motion in a cosmological setting provided we are studying a loop or a segment on a long string which is much smaller than the horizon.

To study the motion of strings we use the Nambu-Goto action [17, 18] which is proportional to the area of the string world-sheet. Minimising this action in the gauge where

$$\partial_u x^\mu \partial_u x_\mu = \partial_v x^\mu \partial_v x_\mu = 0. \quad (1)$$

yields the wave equation for the string

$$\partial_u \partial_v x^\mu(u, v) = 0. \quad (2)$$

The coordinates  $u$  and  $v$  are null on the string world-sheet and typically given in the literature as  $u = t - \sigma$  and  $v = t + \sigma$ , where  $t$  is the time coordinate and  $\sigma$  is a spatial parameter that measures energy density along the string. The constraint Eqs. (1), leave some residual freedom which can be removed by imposing  $a^0 = u$  and  $b^0 = v$ .

The general solution to Eq. (2) can be therefore be written as

$$\mathbf{x}(\sigma, t) = \frac{1}{2}[\mathbf{a}(t - \sigma) + \mathbf{b}(t + \sigma)] \quad (3)$$

and the constraint Eqs. (1) become

$$\mathbf{a}'^2 = \mathbf{b}'^2 = 1, \quad (4)$$

where  $\mathbf{a}'$  and  $\mathbf{b}'$  are the derivatives of  $\mathbf{a}$  and  $\mathbf{b}$  with respect to their arguments,  $t - \sigma$  and  $t + \sigma$  respectively. These vectors therefore live on a unit sphere [19] and will be referred to as the right- and left-moving halves of the string.

Expressions for the functions  $\mathbf{a}'$  and  $\mathbf{b}'$  are most easily written as sums of Fourier harmonics. Unfortunately the

unit magnitude constraint Eq. (4) generally gives a non-linear set of equations involving the vector coefficients of the Fourier expansion and parametrising strings beyond the first few harmonics proves to be analytically intractable. There exists a method to generate strings involving products of rotation matrices that greatly simplifies this task [20]. In this method the  $\mathbf{a}'$  and  $\mathbf{b}'$  are generated by starting with a unit vector and operating on it with a series of rotation matrices that through trigonometric identities produce harmonics. The advantage of using this method to generate loops is that the unit magnitude constraint on the right- and left-movers is satisfied trivially.

As an example of this method we can define the following loop

$$\mathbf{a}'(u) = R_{xy}(\alpha)R_{yz}\left(\frac{2\pi n}{L}u\right)\hat{z}, \quad \mathbf{b}'(v) = R_{xz}\left(\frac{2\pi m}{L}v\right)\hat{z}, \quad (5)$$

where  $R_{ij}(\gamma)$  is a 3-dimensional rotation matrix that rotates the  $i$ - $j$  plane by an angle  $\gamma$ ; the direction of the rotation is chosen such that the positive end of the  $i$ th axis is rotated toward the positive end of the  $j$ th axis. On the unit sphere,  $\mathbf{a}'$  as given by Eq. (5) is a unit circle which is tilted away from the  $y$ - $z$  plane by an angle  $\alpha$ . Similarly  $\mathbf{b}'$  is a unit circle on the  $x$ - $z$  plane. This loop is (aside from an overall spatial rotation) identical to the family of loops introduced by Burden [21].

Another advantage of the method of products of rotations is that it lends itself readily to modifications of the loop trajectory. It is particularly easy to introduce helical perturbations in one or both directions. If we examine Eq. (5) we observe that both  $\mathbf{a}'$  and  $\mathbf{b}'$  consist of a rotation of the unit vector  $\hat{z}$  on some plane. To introduce helical perturbations in, say,  $\mathbf{b}'$ , we can replace the starting unit vector with

$$\hat{z} \rightarrow \hat{z}' = (1 - \epsilon_b^2)^{1/2}\hat{z} + \epsilon_b R_{xy}\left(\frac{2\pi l_b}{L}v\right)\hat{x}, \quad (6)$$

with  $\epsilon_b < 1$  and then subject this new unit vector to a rotation on the same plane as before, namely,

$$\begin{aligned} \mathbf{b}'(v) &= R_{xz}\left(\frac{2\pi m}{L}v\right)\hat{z}' \\ &= R_{xz}\left(\frac{2\pi m}{L}v\right)\left((1 - \epsilon_b^2)^{1/2}\hat{z} + \epsilon_b R_{xy}\left(\frac{2\pi l_b}{L}v\right)\hat{x}\right). \end{aligned} \quad (7)$$

The unit vector given by Eq. (6) consists of two parts. The first part is a vector of magnitude  $(1 - \epsilon_b^2)^{1/2}$  in the direction of  $\hat{z}$  and it corresponds to the straight part of  $\mathbf{b}'$ . The second part is a circle of radius  $\epsilon_b$  on the  $x$ - $y$  plane, perpendicular therefore to  $\hat{z}$ , that winds around this plane  $l_b$  times. This represents the perturbed part of  $\mathbf{b}'$ . Acting on this new unit vector  $\hat{z}'$  with the rotation  $R_{xz}\left(\frac{2\pi m}{L}v\right)$  produces a curve in the unit sphere with helical perturbations of radius  $\epsilon_b$ . An analogous operation can be carried out on  $\mathbf{a}'$ .

Figure 1 illustrates the effect of this procedure. Equation (5) gives  $\mathbf{a}'$  and  $\mathbf{b}'$  that trace out great circles on the

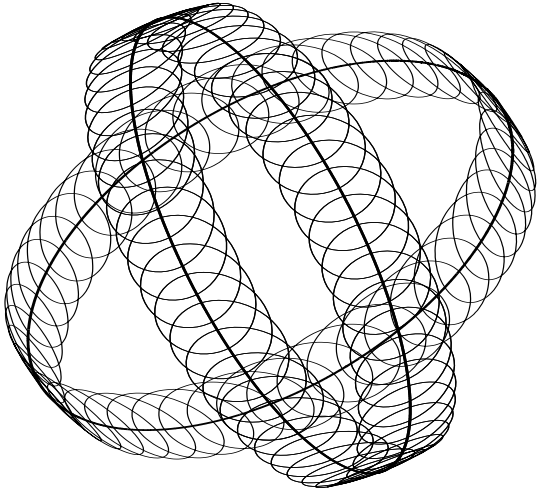


FIG. 1: Right and left movers on the unit sphere. The thicker curves that encircle the sphere once correspond to  $\mathbf{a}'$  and  $\mathbf{b}'$  as given by Eq. (5) with  $\alpha = 0$ ,  $n = 1$  and  $m = 2$ . The complex curves correspond to the perturbed versions of  $\mathbf{a}'$  and  $\mathbf{b}'$  with  $\epsilon_a = \epsilon_b = 0.2$ ,  $l_a = 100$  and  $l_b = 200$ . We have introduced twice as many oscillations in the perturbation for  $\mathbf{b}'$  because the unperturbed  $\mathbf{b}'$  winds twice around the unit sphere.

unit sphere. Perturbations from Eq. (7) and its analog for  $\mathbf{a}'$  add small, circular oscillations to the larger loops.

### III. THE FORMS OF COSMIC STRING CUSPS IN THE PRESENCE OF SMALL-SCALE STRUCTURE

Cusps are regions on long strings or loops that achieve phenomenal Lorentz boosts. These boosts, combined with the potentially large mass per unit length of cosmic strings, may lead to the production of a detectable gravitational wave signal [5].

Cusps arise when the right- and left-moving parts of the string cross on the unit sphere. At the crossing they point in the same direction, namely,

$$\mathbf{a}' = \mathbf{b}'. \quad (8)$$

In this case

$$\mathbf{x}' = \frac{1}{2}[-\mathbf{a}' + \mathbf{b}'] = 0, \quad (9)$$

and

$$\dot{\mathbf{x}} = \frac{1}{2}[\mathbf{a}' + \mathbf{b}'] = \mathbf{a}' = \mathbf{b}'. \quad (10)$$

Here  $\mathbf{x}' = \partial_\sigma \mathbf{x}$  and  $\dot{\mathbf{x}} = \partial_t \mathbf{x}$ . The tip of the cusp therefore moves at the speed of light and a small region of string

around the cusp has an enormous Lorentz boost. Cusps are generic in the sense that the  $\mathbf{a}'$  and  $\mathbf{b}'$  are confined to live on the unit sphere and for general string and loop configurations we typically expect them to cross.

The effects on cusps of the presence of small-scale structure on just one of the string halves (‘chiral’ structure) was investigated briefly in [22]. There it was argued that the shape of the cusp depends on the contribution of the small perturbations to the effective mass per unit length of the string. Here we will review and expand that discussion to the more general case of small-scale structure on both halves of the string. Although the detailed properties of small-scale structure in cosmic string networks are still not understood it is useful to study the range of possibilities. Below we show that under most circumstances the presence of small-scale structure at a cusp leads to the formation of loops at the size of the smallest scales.

For simplicity we consider a loop of size  $L$  with small-scale structure of wavelength  $\lambda$  and amplitude to wavelength ratio  $\epsilon$ . For now we take the small-scale structure to be the same in both directions. The string has an effective thickness due to the small-scale structure,

$$d \sim 2\epsilon\lambda. \quad (11)$$

When a long string or loop has a cusp the effective thickness of the string may result in overlap. Calculations for the overlap of the fields making up the string core have been performed in [23] and [24]. In the case of core overlap the fields in a small section of the string near the tip of the cusp unwind and produce energy in the form of particles, the bosons that make up the string. Fortunately we can borrow these results, expecting, however, for overlap to result in the formation of cosmic string loops rather than particles. The latter work [24] took account of the Lorentz contraction of the core and is the correct calculation for generic string core overlap. The former work [23] did not account for the contraction of the string core but, as we will see, the main result may be useful in the case of back-reaction-dominated cusps.

If the small-scale structure is small enough to have little effect on the average motion of the string, then the analysis of [24] applies, and we expect an overlapping region near the cusp of length

$$l \sim \sqrt{dL} \quad (12)$$

which will typically fragment into about  $\sqrt{\epsilon L/\lambda}$  relativistic loops of the small-scale size  $\lambda$ . Here the effect of the small-scale structure has been to replace the core thickness of the string with the effective thickness  $d$ , which is usually much larger.

The overlap begins when the Lorentz gamma factor of the cusp reaches the value

$$\gamma_0 \sim \sqrt{L/d}. \quad (13)$$

When the small-scale structure is not symmetrically distributed between the right- and left-movers at the cusp,

the overlap expressions, Eqs. (12) and (13), will be dominated by the larger of the two halves.

On the other hand, if the small-scale structure is large enough, there will be important corrections to the Nambu-Goto motion. The effect of small-scale structure increases as the string begins to move rapidly near a cusp, with the effective mass per unit length becoming

$$\mu_{\text{eff}} = \mu(1 + \gamma^2 \epsilon^2). \quad (14)$$

Therefore when the gamma factor reaches the value

$$\gamma_b \sim 1/\epsilon \quad (15)$$

the contribution to the effective mass per unit length of the string becomes significant and the effective motion of the string deviates from regular Nambu-Goto motion. Averaging the motion of the string over scales of the size of the small-scale structure and smaller results in an increase of the effective mass density and a decrease of the tension of the string [25].

Whether back-reaction prevents the formation of the relativistic cusp depends on which one of the two gamma factors, Eq. (15) or Eq. (13), is the smallest. If  $\epsilon^2 L/d < 1$ , then  $\gamma_b > \gamma_0$ , and overlap begins before back-reaction is important. On the other hand, if  $\epsilon^2 L/d > 1$ , then back-reaction changes the form of the cusp.

The simplest situation of the latter sort occurs when both string halves contribute equally to the effective mass per unit length. Then the effective motion of the string is given by [2]

$$\mathbf{x}(\sigma, t) = \frac{1}{2}[\mathbf{a}(k\sigma) + \mathbf{b}(k\sigma)] \quad (16)$$

with  $k = \sqrt{1 - \epsilon^2}$ . The two halves therefore live on a sphere of radius  $k < 1$ . Sharp cusps form as before, because at crossings on the sphere the effective  $\dot{\mathbf{x}} = 0$ , but the tips of cusps move at a speed  $|\dot{\mathbf{x}}| = k$  rather than at the speed of light. Because the cusps are sharp we expect the small-scale structure to overlap. If the perturbations are small then the cusp is relativistic and we expect an overlapping region around the cusp of a size given by Eq. (12) and the production of relativistic loops. However, if the small-scale structure is sufficiently large the region of overlap will be larger due to the negligible Lorentz contraction of the core and we can use the result in [23]. In this case we expect an overlapping region of size

$$l \sim d^{1/3} L^{2/3} \quad (17)$$

around the cusp, which will fragment into about  $\epsilon^{1/3}(L/\lambda)^{2/3}$  loops of the small-scale size  $\lambda$ . Since the loops produced in this case are non-relativistic, this mechanism may be responsible for the large number of small loops seen in simulations.

At first glance the small-scale structure in numerical simulations would appear too small to slow down cusps sufficiently to produce non-relativistic loops. However,

the wavelength of the perturbations on long strings is a very small fraction of the length of the long strings and the fact that it can be observed at all in simulations means the amplitude to wavelength ratios cannot be negligibly small.

If the small-scale structure is not symmetrically distributed between the right- and left-movers at the cusp, for example because of statistical fluctuations, the radii of the spheres on which the effective right- and left-moving halves live will be different. They will therefore miss each other and make  $\mathbf{x}'$  finite, with

$$|\mathbf{x}'| \sim |k_b - k_a| \sim |\epsilon_a^2 - \epsilon_b^2| \quad (18)$$

at the cusp. Here, the sub-indices  $a$  and  $b$  distinguish between right- and left-movers. The limiting situation of ‘chiral’ small-scale structure (i.e.,  $\epsilon_b = 0$ ) was investigated in [22] and is similar to that of a superconducting string with a chiral neutral current [26, 27].

Since  $\mathbf{x}'$  is finite the cusp will be rounded. If the radius of curvature of the cusp is comparable to the effective thickness of the string then we are in the same situation as before: a section of string will overlap near the cusp. The amount of overlap will be given by either one of Eqs. (12) or (17) depending on the size of the small-scale structure.

If the radius of curvature of the cusp is much larger than the thickness then there will be no overlap. This case is analogous to that of superconducting strings with a chiral neutral current and we expect self-intersections to occur at the cusp about half of the time [28]. These self-intersections result in the production of a loop of size

$$l \sim |\epsilon_a^2 - \epsilon_b^2|^{1/2} L \quad (19)$$

which will fragment into about  $|\epsilon_a^2 - \epsilon_b^2|^{1/2} L/\lambda$  loops of the small-scale size  $\lambda$ .

To summarise, we have seen that in most cases overlap of the small-scale structure at a cusp leads to the formation of loops at the smallest scales. The only exception occurs when the small-scale structure is a) sufficiently large that the averaged motion of the string deviates significantly from Nambu-Goto motion, and b) sufficiently asymmetric that the radius of curvature of the cusp is larger than the effective thickness of the string. Even in this case, however, we expect intersections to produce small loops about half the time.

Figure 2 illustrates the various possibilities for the shape of cusps with small-scale structure described above. Without small-scale structure, we have a sharp cusp which would evaporate at the tip by core overlap. With symmetrical small excitations, the cusp is still sharp and will chop off a loop by the overlap of the wiggles. With asymmetrical small-scale structure, the cusp will be smoothed out. There may or may not be an intercommutation, depending on which half of the string has the larger perturbations, as discussed in [28].

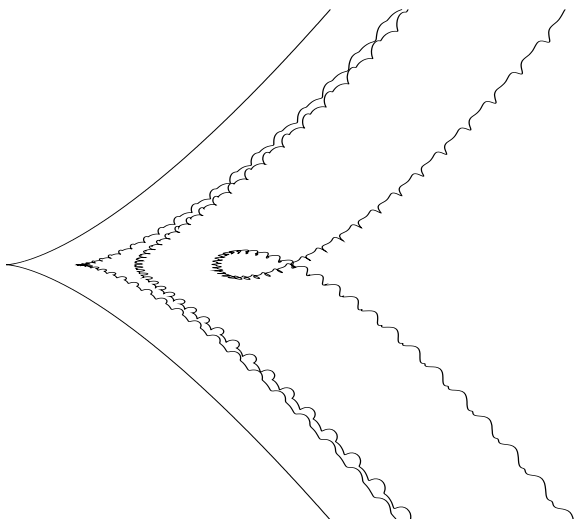


FIG. 2: On the left, a projection of an unperturbed cusp on a loop given by Eq. (5) with  $\alpha = 0$ ,  $n = 1$  and  $m = 2$ . Next to the right, a perturbed version of the same cusp with  $\epsilon_a = \epsilon_b = 0.3$ ,  $l_a = 200$  and  $l_b = 400$ . Next a projection of a cusp with  $\epsilon_a = 0.4$ ,  $\epsilon_b = 0.5$ ,  $l_a = 200$  and  $l_b = 400$ . In this case the effective  $\mathbf{x}'$  is finite and the cusp is smoothed out. On the right, a cusp with  $n = 2$ ,  $m = 1$ ,  $\epsilon_a = 0.4$ ,  $\epsilon_b = 0.5$ ,  $l_a = 200$  and  $l_b = 400$ . Switching the values of  $n$  and  $m$  has inverted the sign of  $\mathbf{x}'$  and led to a self-intersection near the cusp.

#### IV. GRAVITATIONAL WAVEFORMS: FORMALISM AND NUMERICAL IMPLEMENTATION

Periodic sources produce a metric perturbation that in the wave-zone is given by a sum of plane waves [29]

$$h_{\mu\nu}(\mathbf{x}, t) = \sum_{n=-\infty}^{\infty} \epsilon_{\mu\nu}^{(n)}(\mathbf{x}, \omega_n) e^{-ik_n \cdot x}. \quad (20)$$

The polarisation tensor  $\epsilon_{\mu\nu}^{(n)}$  is given by

$$\epsilon_{\mu\nu}^{(n)}(\mathbf{x}, \omega_n) = \frac{4G}{r} (T_{\mu\nu}(k_n) - \frac{1}{2} \eta_{\mu\nu} T_\lambda^\lambda(k_n)) \quad (21)$$

and

$$T^{\mu\nu}(k_n) = \frac{1}{T} \int_0^T dt \int d^3\mathbf{x} T^{\mu\nu}(x) e^{ik_n \cdot x} \quad (22)$$

is the Fourier transform of the stress-energy tensor of the source. In these expressions  $r$  is the distance to the source,  $T$  is the period of motion,

$$k_n^\mu = \omega_n(1, \hat{\Omega}) \quad (23)$$

is the wave-vector of the gravitational wave,  $\hat{\Omega}$  is a unit vector pointing from the source to the point of observation and  $\omega_n = 2\pi n/T$  is the frequency.

In the gauge defined by Eq. (4) the stress energy tensor of the string can be put in the form

$$T^{\mu\nu}(x) = \mu \int dudv (x_{,u}^\mu x_{,v}^\nu + x_{,u}^\nu x_{,v}^\mu) \delta^{(4)}(x - x(\zeta)). \quad (24)$$

We consider a loop of length  $L$  which oscillates periodically with period  $T = L/2$ . The Fourier transform of the stress-energy tensor of the loop is

$$T^{\mu\nu}(k_n) = \frac{2\mu}{L} \int_0^{L/2} dt \int d^3\mathbf{x} e^{ik_n \cdot x} \int dudv \times [x_{,u}^\mu x_{,v}^\nu + x_{,u}^\nu x_{,v}^\mu] \delta^{(4)}(x - x(u, v)). \quad (25)$$

The expression for the string position in terms of right- and left-moving parts when substituted in Eq. (25) yields the symmetrised product

$$T^{\mu\nu}(k_n) = \frac{\mu L}{2} (A^\mu(k_n) B^\nu(k_n) + A^\nu(k_n) B^\mu(k_n)), \quad (26)$$

where

$$A^\mu(k_n) = \frac{1}{L} \int_0^L du a'^\mu(u) e^{ik_n \cdot a(u)/2}, \quad (27)$$

and

$$B^\mu(k_n) = \frac{1}{L} \int_0^L dv b'^\mu(v) e^{ik_n \cdot b(v)/2}. \quad (28)$$

This means that we can write the polarisation tensor Eq. (21) as

$$\epsilon_{\mu\nu}^{(n)}(\mathbf{x}, \omega_n) = \frac{2G\mu L}{r} [A_\mu(k_n) B_\nu(k_n) + A_\nu(k_n) B_\mu(k_n) - \eta_{\mu\nu} A_\lambda(k_n) B^\lambda(k_n)]. \quad (29)$$

We are free to choose coordinates such that the wave-vector lies on the  $z$ -axis. In this case the only physical components of the polarisation tensor can be shown to be  $\epsilon_{11}^{(n)} \equiv \epsilon_+^{(n)}$  and  $\epsilon_{12}^{(n)} \equiv \epsilon_\times^{(n)}$  [29], which are referred to as the  $+$ - and  $\times$ -polarisations of the gravitational wave [30].

It is easy to show using integration by parts and the periodicity of  $a^\mu$  and  $b^\mu$  that

$$k_n^\mu A_\mu(k_n) = k_n^\mu B_\mu(k_n) = 0. \quad (30)$$

Using this identity and Eq. (29) one finds that the amplitudes of the  $+$ - and  $\times$ -polarised waves are given by

$$\epsilon_+^{(n)} = \frac{2G\mu L}{r} (A_x(k_n) B_x(k_n) - A_y(k_n) B_y(k_n)) \quad (31)$$

and

$$\epsilon_\times^{(n)} = \frac{2G\mu L}{r} (A_x(k_n) B_y(k_n) + A_y(k_n) B_x(k_n)) \quad (32)$$

respectively.

The metric perturbation can therefore be written as

$$h_{+/\times}(\mathbf{x}, t) = \sum_{n=-\infty}^{\infty} \epsilon_{+/\times}^{(n)}(\mathbf{x}, \omega_n) e^{-ik_n \cdot x}. \quad (33)$$

The  $n=0$  mode in this sum corresponds to the static field and should not be included in the sum if we are interested in the radiative part of the metric perturbation.

In order to study the gravitational waveforms produced by arbitrary loops we must resort to numerical methods. If we consider a loop composed of some continuous functions  $\mathbf{a}(u)$  and  $\mathbf{b}(v)$  we can always approximate it by choosing some discretisation scheme that is sufficiently fine so that all the features of the loop are resolved. We can use this discretisation to compute the integrals Eqs. (27) and (28) and find the gravitational waveform it produces.

Here we use the piece-wise linear discretisation [31]. Allen and Ottewill [32] computed the gravitational waveforms for a number of different loop trajectories and showed that in the piece-wise linear approximation the waveform for those loops is in good agreement with their analytic calculations. Furthermore, as they found, an advantage of using this particular approximation in the calculation of gravitational waveforms is that the integrals Eqs. (27) and (28) can be performed exactly. This result is computed explicitly below.

In the piece-wise linear discretisation both functions  $\mathbf{a}(u)$  and  $\mathbf{b}(v)$  are constructed out of  $N_a$  and  $N_b$  straight segments joined at kinks. The values of the internal parameters  $u$  and  $v$  are continuous and are labeled by  $u_j$  with  $j = 0, 1, \dots, N_a - 2, N_a - 1$ , and a similar expression for  $v_j$ , at the kinks. Here we will take  $N_a = N_b = N$  and space the internal parameters evenly between the kinks ( $u_{j+1} - u_j = v_{k+1} - v_k = \delta$  for all  $j$  and  $k$ ) for simplicity. The functions  $\mathbf{a}(u)$  and  $\mathbf{b}(v)$  are defined at the kinks

$$\mathbf{a}_j = \mathbf{a}(u_j), \quad \mathbf{b}_k = \mathbf{b}(v_k) \quad (34)$$

and the derivatives of these functions in the intervening straight segments between the kinks

$$\mathbf{a}'_j = \frac{\mathbf{a}_{j+1} - \mathbf{a}_j}{\delta}, \quad \mathbf{b}'_k = \frac{\mathbf{b}_{k+1} - \mathbf{b}_k}{\delta}. \quad (35)$$

Here we will focus only on  $A^\mu(k_n)$  because the situation for  $B^\mu(k_n)$  is completely analogous. For piece-wise linear loops the integral of  $A^\mu(k_n)$  in Eq. (27) becomes a sum of integrals between kinks

$$A^\mu(k_n) = \frac{1}{L} \sum_{j=0}^{N-1} a_j'^\mu \int_{u_j}^{u_{j+1}} du e^{ik_n \cdot a(u)/2}. \quad (36)$$

Since the string segments are taken to be straight between the kinks

$$a^\mu(u) = a_j^\mu + (u - u_j) a_j'^\mu, \quad (37)$$

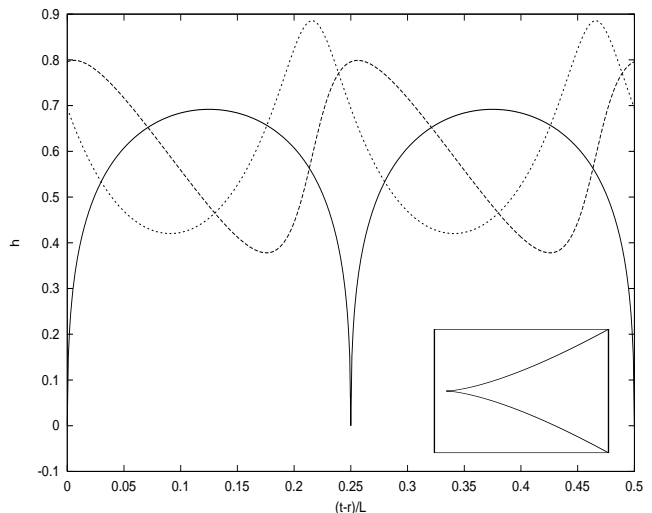


FIG. 3: Waveforms for the loop defined by Eq. (5) with  $\alpha = 0$ ,  $n = 1$  and  $m = 2$ , whose cusp is shown in the inset and first in Figure 2, as a function of time. The solid line is the  $\times$ -polarised waveform when looking straight at the cusp in the  $z$ -direction. No gravity wave is emitted with  $+$  polarisation in this direction. For the same loop with an overall spatial rotation of 1 radian about the  $x$ -axis, so that we are looking off-cusp, the  $+-$ polarised waveform is dashed and the  $\times$ -polarised waveform is dotted. All waveforms are summed over the first 2000 Fourier modes with  $2G\mu L/r = 1$ . The loop is approximated with 5000 linear segments giving a resolution of the internal parameters  $\delta = 2 \times 10^{-4} L$ .

the integrand in Eq. (36) is a simple exponential. From here it is straightforward to show that

$$A^\mu(k_n) = \sum_{j=0}^{N-1} \frac{2a_j'^\mu}{iL\omega_n(1 - \hat{\Omega} \cdot \mathbf{a}'_j)} \times [e^{i\omega_n(u_{j+1} - \hat{\Omega} \cdot \mathbf{a}_{j+1})/2} - e^{i\omega_n(u_j - \hat{\Omega} \cdot \mathbf{a}_j)/2}] \quad (38)$$

with a similar expression for  $B^\mu(k_n)$ .

## V. GRAVITATIONAL WAVEFORMS FROM CUSPS

Gravitational bursts produced by cusps have previously been studied analytically by Damour and Vilenkin [5]. They found the metric perturbation produced by a cusp to be

$$h(t) \propto |t - r|^{1/3} \quad (39)$$

where  $r$  is the distance to the source.

As an example we can check waveform of a cusp on a loop. We take the loop defined by Eq. (5) which has a cusp in the  $z$ -direction at  $t = 0$  and  $t = L/4$ . The on- and off-cusp waveforms for this loop are shown in Figure 3 for  $\alpha = 0$ ,  $n = 1$  and  $m = 2$ .

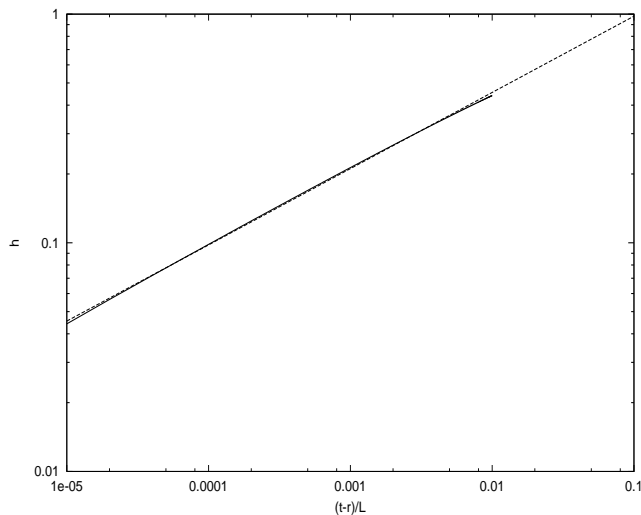


FIG. 4: Log-log plot of the cusp waveform for the loop defined by Eq. (5) with  $\alpha = 0$ ,  $n = 1$  and  $m = 2$  as a function of time. The solid curve gives the  $\times$ -polarised waveform computed numerically and the dashed curve is given by Eq. (40) with  $a = 2.11$  (fit to the data). The waveform has been summed over the first  $2 \times 10^7$  Fourier modes with  $2G\mu L/r = 1$ .

Figure 4 shows a log-log plot of the waveform versus time near the cusp. The solid curve gives the waveform computed numerically over the first  $2 \times 10^7$  Fourier modes, with  $2G\mu L/r = 1$  and the dashed curve is given by

$$h_{\times} = a |t - r|^{1/3} \quad (40)$$

with  $a = 2.11$  (fit to the data). The large number of Fourier modes necessary to reproduce the behaviour of Eq. (39) is due to the slow decrease in amplitude of  $h_{\times}$  as a function of the Fourier mode,  $h_{\times}(n) \propto n^{-4/3}$ .

Due to the pervasiveness of small-scale structure in numerical simulations of cosmic strings, it is important to test the robustness of the prediction for the gravitational waveform of a cusp, Eq. (39), to the presence of small-scale structure.

In order to investigate the effects of small-scale structure on the gravitational waveforms of cusps we have performed a number of simulations of cosmic string loops with small perturbations. Figures 5–7 show the waveforms of the loops whose cusps appear in Figure 2. The waveforms are computed by summing over the first 10000 Fourier modes with  $2G\mu L/r = 1$ . The loops are approximated with 5000 linear segments. Intercommutations are not performed in the simulation; the strings just pass through each other without producing new loops.

These figures show that the overall shape of the waveform of the cusp is not greatly affected by the presence of small-scale structure even when the amplitude of the small-scale structure  $\epsilon$  is not particularly small. The primary effect is to smooth out the very sharp point in the waveform. But that point is visible only if the observer is located in the direction of cusp motion. Gravity waves

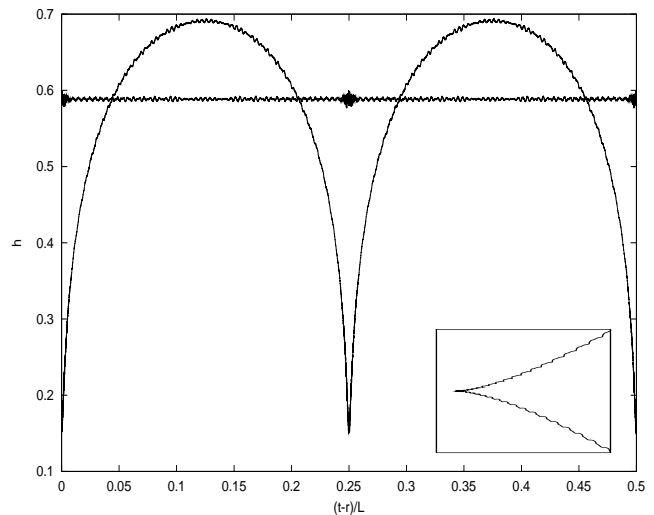


FIG. 5: Waveforms for a perturbed loop, given by  $\alpha = 0$ ,  $n = 1$ ,  $m = 2$ ,  $\epsilon_a = \epsilon_b = 0.3$ ,  $l_a = 200$  and  $l_b = 400$ , whose cusp is shown second in Figure 2 and in the inset, looking straight at the cusp in the  $z$ -direction. Because of the perturbations there is now a small  $+$ -polarised wave and the form of the  $\times$ -polarised wave is not as sharp as in Figure 3.

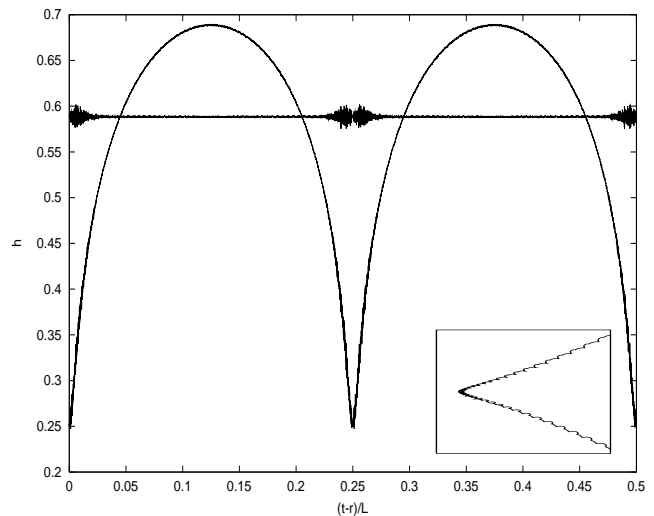


FIG. 6: Waveforms for a perturbed loop with  $\alpha = 0$ ,  $n = 1$ ,  $m = 2$ ,  $\epsilon_a = 0.4$ ,  $\epsilon_b = 0.5$ ,  $l_a = 200$  and  $l_b = 400$ , whose cusp is shown third in Figure 2 and in the inset.

emitted from the string moving with Lorentz boost  $\gamma$  are confined to a cone with angle  $\theta \sim \gamma^{-1}$  [5]. The smoothing of the sharp waveform is due primarily to the limitation of the string boost at  $\gamma_b$ , so the change in the waveform will be observed only if one is within angle  $\gamma_b^{-1} \sim \epsilon$  of the direction of cusp motion.

In addition to the smoothing of the large cusp the waveforms also show significant sub-structure. It is a result of the small helical perturbations and is present in both the  $+$ -polarised and  $\times$ -polarised waveforms.

The sub-structure is particularly prominent at the time

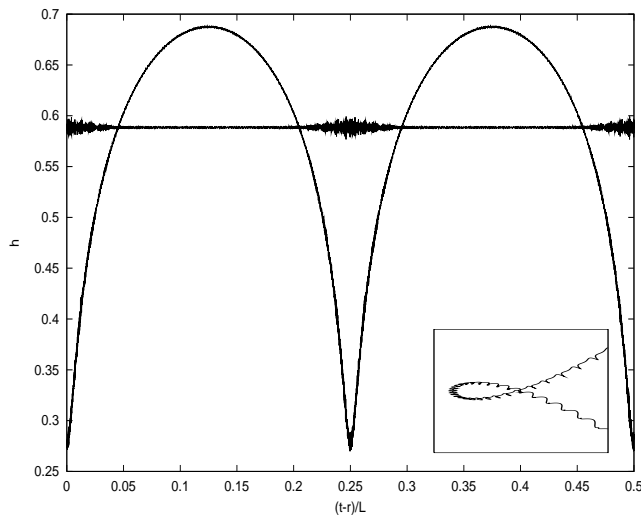


FIG. 7: Waveforms for a perturbed loop with  $\alpha = 0$ ,  $n = 2$ ,  $m = 1$ ,  $\epsilon_a = 0.4$ ,  $\epsilon_b = 0.5$ ,  $l_a = 200$  and  $l_b = 400$ , whose cusp is shown last in Figure 2 and in the inset.

the large cusp forms and corresponds to the waveforms of many tiny cusps. These smaller cusps form as a result of the crossings on the unit sphere that occur around the time the large cusp forms (as in Figure 1). In terms of gravitational wave detection it is possible that the small scale structure gives the dominant contribution to the waveform in some range of frequencies. This possibility depends on the value of  $G\mu$  and the details of cosmic string network evolution and deserves further investigation.

## VI. CONCLUSIONS

The presence of small-scale structure at cusps leads to a multitude of interesting behaviours mostly involving self-intersections of the loop or long string that produces the cusp. The specific processes and outcomes depend on the detailed properties of the small-scale structure. Indeed, one of the scenarios presented here supports the ideas of Albrecht [13] who first suggested that the small loops seen in simulations are produced at cusps.

At first glance it would appear that cusps are only able to produce ultra-relativistic loops, which would rule out this mechanism since such loops are not seen in simulations. However, in the regime where the small-scale structure has enough amplitude to significantly affect the motion of the string, the cusp and the loops it produces through overlap will no longer be relativistic.

As an illustration we take the canonical value for the size of the small-scale structure, which for GUT strings is  $\lambda \sim 10^{-4}t$ , and a significant amplitude to wave-length ratio,  $\epsilon \sim 1$ . Then we expect a horizon-sized cusp, of size  $L \sim t$ , to produce a few hundred non-relativistic loops

$$\epsilon^{1/3}(L/\lambda)^{2/3} \sim 500. \quad (41)$$

The primary effect of small-scale structure is to smooth out the sharp waveform emitted by the large cusp in the direction of its motion. That waveform is smoothed anyway if one is located away from the exact direction of motion; observers outside a cone whose angle is proportional to the small-scale structure amplitude will see little change. However, since superimposed on the large cusp there is a multitude of smaller ones, it may be that the small-scale structure turns out to give the dominant contribution to the gravitational wave signal in the range of frequencies onto which we happen to have our observational window. This depends on the typical size of loops and the spectrum of perturbations that ends up on loops. This possibility deserves further investigation.

Unfortunately, the uncertainties that remain regarding string network evolution make it difficult to say anything definite in this regard. For instance, if it turns out to be correct that most loops are produced at the smallest possible scales then we do not expect them to have any significant structure.

## Acknowledgments

We would like to thank Alex Vilenkin for very helpful discussions and suggestions and Bruce Allen and A. Ottewill for useful and friendly correspondence. K. D. O. was supported in part by the National Science Foundation. X. S. was supported by National Science Foundation grants PHY 0071028 and PHY 0079683.

- 
- [1] T.W.B. Kibble, *J. Phys.* **A9** (1976) 1387.
  - [2] A. Vilenkin and E.P.S. Shellard, *Cosmic strings and other Topological Defects*. Cambridge University Press, 2000; M. Hindmarsh and T.W.B. Kibble, *Rept. Prog. Phys.* **58** (1995) 477.
  - [3] S. Sarangi, and S.H. Tye, *Phys. Lett.* **B536** (2002) 185.
  - [4] V. Berezhinsky, B. Hnatyk and A. Vilenkin, *Phys. Rev.* **D64** (2001) 043004.
  - [5] T. Damour and A. Vilenkin, *Phys. Rev. Lett.* **85** (2000) 3761.
  - [6] P. Bhattacharjee and G. Sigl, *Phys. Rep.* **327** (2000) 109.
  - [7] T.W.B. Kibble, *Nucl. Phys.* **B252** (1985) 227.
  - [8] D.P. Bennett, *Phys. Rev.* **D33** (1986) 872;
  - [9] A. Albrecht and N. Turok, *Phys. Rev.* **D40** (1989) 973.
  - [10] D.P. Bennett and F.R. Bouchet, *Phys. Rev.* **D41** (1990) 2408.
  - [11] B. Allen and E.P.S. Shellard, *Phys. Rev. Lett.* **64** (1990) 119.
  - [12] B. Allen and R. Caldwell, *Phys. Rev.* **D43** (1991) 3173.
  - [13] A. Albrecht, *The Formation and Evolution of Cosmic Strings*. G. Gibbons, S. Hawking and T. Vachaspati, Eds. Cambridge University Press, 1989.



- [14] D.P. Bennett and F.R. Bouchet, Phys. Rev. Lett. 60 (1988) 257.
- [15] X. Siemens, K.D. Olum and A. Vilenkin, Phys. Rev. **D66** (2002) 043501.
- [16] A. Vilenkin, Phys. Lett. **B107** (1981) 47.
- [17] Y. Nambu, Proceedings of Int. Conf. on Symmetries and Quark Models. Wayne State University. Takinawa, 1969.
- [18] T. Goto, Prog. Theor. Phys. 46 (1971) 1560.
- [19] T.W.B. Kibble and N. Turok, Phys. Lett. **B116** (1982) 141.
- [20] R.W. Brown and D.B. DeLaney, Phys. Rev. Lett. 63 (1989) 474; R.W. Brown, M.E. Convery and D.B. DeLaney, J. Math. Phys. 32 (1991) 1674.
- [21] C.J. Burden, Phys. Lett. **B164** (1985) 277.
- [22] X. Siemens and K.D. Olum, Nucl. Phys **B611** (2001) 125; Erratum-ibid. **B645** (2002) 367.
- [23] R.H. Brandenberger, Nucl.Phys. **B293** (1987) 812.
- [24] J.J. Blanco-Pillado and K.D. Olum, Phys. Rev. D59 (1999) 063508.
- [25] B. Carter, Phys. Rev. D41 (1990) 3869.; A. Vilenkin, Phys. Rev. D41 (1990) 3038
- [26] B. Carter and P. Peter, Phys. Lett. **B466** (1999) 41.
- [27] J.J. Blanco-Pillado, K.D. Olum and A. Vilenkin, Phys. Rev. **D 63** (2001) 103513.
- [28] K.D. Olum, J.J. Blanco-Pillado, X. Siemens, Nucl.Phys. **B599** (2001) 446.
- [29] S. Weinberg, Gravitation and Cosmology. John Wiley and Sons, 1972.
- [30] C.W. Misner, K.S. Thorne and J.A. Wheeler, Gravitation. Freeman, 1970.
- [31] B. Allen and P. Casper, Phys. Rev. **D50** (1994) 2496.
- [32] B. Allen and A.C. Ottewill, Phys. Rev.**D63** (2001) 063507.